bioRxiv preprint doi: https://doi.org/10.1101/175489; this version posted August 11, 2017. The copyright holder for this preprint (which was not certified by peer review) is the author/funder, who has granted bioRxiv a license to display the preprint in perpetuity. It is made available under aCC-BY-NC-ND 4.0 International license.

Common variants of *NRXN1*, *LRP1B* and *RORA* are associated with increased ventricular volumes in psychosis - GWAS findings from the B-SNIP deep phenotyping study

AUTHORS:
Alliey-Rodriguez, Ney[1]; Grey, Tamar A[2]; Shafee, Rebecca[3a,4]; Padmanabhan, Jaya[3]; Tandon, Neeraj[3]; Klinger, Madeline[1]; Spring, Jonathan[1a]; Coppes, Lucas[1]; Reis, Katherine[1]; Keshavan, Matcheri S[3];Gage, Diane[4]; McCarroll, Steven[4]; Bishop, Jeffrey R[5]; Hill, Scot[6]; Reilly, James L[7]; Lencer, Rebekka[8]; Clementz, Brett[9]; Buckley, Peter[10]; Meda, Shashwath[11]; Narayanan, Balaji[11]; Glahn, David C[11]; Pearlson, Godfrey[11]; Ivleva, Elena I[12]; Tamminga, Carol[12]; Sweeney, John A[12]; Curtis, David [13]; Keedy, Sarah[1]; Badner, Judith A[14]; Liu, Chunyu[15]; Gershon, Elliot S[1,1b].

Affiliations: [1]University of Chicago, Department of Psychiatry and Behavioral Neurosciences; [1a]University of Chicago Laboratory for Advanced Computing; [1b]University of Chicago, Department of Human Genetics; [2]Massachusetts Institute of Technology; [3]Harvard Medical School, Department of Psychiatry; [3a]Harvard Medical School, Department of Genetics [4]Broad Institute of MIT and Harvard; [5]University of Minnesota, Department of Experimental and Clinical Pharmacology; [6]Rosalind Franklin University; [7]Northwestern University; [8]University of Muenster; [9]Department of Psychology, University of Georgia, Athens; [10] Virginia Commonwealth University; [11]Yale University Departments of Psychiatry & Neuroscience; [12]University of Texas Southwestern Medical Center, Department of Psychiatry; [13]University College London and Centre for Psychiatry, Barts and the London School of Medicine and Dentistry; [14]Rush University Medical Center; [15]University of Illinois at Chicago.

ABSTRACT:

Schizophrenia, Schizoaffective, and Bipolar Disorders share common illness traits, intermediate phenotypes and a partially overlapping polygenic basis. We performed GWAS on deep phenotyping data, including structural MRI and DTI, clinical, and behavioral scales from 1,115 cases and controls. Significant associations were observed with two cerebrospinal fluid volumes: the temporal horn of left lateral ventricle was associated with *NRXN1*, and the volume of the cavum septum pellucidum was associated with *LRP1B* and *RORA*. Both volumes were associated with illness. Suggestive associations were observed with local gyrification indices, fractional anisotropy and age at onset. This is the first report of common genetic variants associated with these intermediate phenotypes.

bioRxiv preprint doi: https://doi.org/10.1101/175489; this version posted August 11, 2017. The copyright holder for this preprint (which was not certified by peer review) is the author/funder, who has granted bioRxiv a license to display the preprint in perpetuity. It is made available under aCC-BY-NC-ND 4.0 International license.

Introduction:

Although very large samples of patients and controls have had genome-wide association studies (GWAS) of diagnosis of psychotic mental disorders[1], the phenotyping has been restricted. There have been very few large- or intermediate-scale studies of the many intermediate phenotypes associated with psychosis. The Bipolar and Schizophrenia Network on Intermediate Phenotypes (B-SNIP) reports here GWAS of deep phenotyping in psychosis, that is, multiple phenotypes on the same individuals, including structural magnetic resonance imaging (MRI), diffusion tensor imaging (DTI), behavioral and clinical phenotypes, from a single cohort of 1,115 individuals, including patients with schizophrenia, schizoaffective, psychotic bipolar disorder, and healthy controls. As noted by Dahl et al. [2], deep phenotyping with simultaneous genome-wide analyses serves as a discovery tool for previously unsuspected relationships of phenotypic traits with each other, and with shared molecular events. Pooling ill subjects with normal controls to analyze quantitative traits has the advantage of a wider range in the observed phenotypes, which translates into higher power to detect genetic associations[3]. All observations were generated and analyzed following standardized procedures, as discussed in prior reports from our consortium [4, 5].

The NIMH Research Domain Criteria (RDoC) initiative (https://www.nimh.nih.gov/research-priorities/rdoc/index.shtml)[6] conceives of dimensional traits that are continuous between patients and controls, and which can serve as a basis for revised definitions of disease traits and categories. In other medical disorders, such as hypertension, genetic variants have been associated with a related quantitative trait (blood pressure), once sample sizes were large enough to detect them [7]. Heritable variance in blood pressure and clinical hypertension are accounted for by GWAS-significant associations with common variants, by polygenic risk, and by rare variants with strong effect[8], which is generally true for common diseases[9].

There is ample evidence of partially overlapping brain morphology abnormalities in schizophrenia (SZ) and bipolar disorder (BD) [10-12]. These disorders also have a shared set of specific genetic loci associated with them, and a partially shared polygenic diathesis [1, 13], as well as shared behavioral features including psychosis in some BD patients. Identifying genetic factors associated with specific biological traits associated with psychosis in these disorders can help to elucidate the biology of shared disease features, which may lead to improved disease classification and personalized treatment [14].

Previous studies have identified enlargement of the ventricular system associated with bipolar disorder and schizophrenia [15, 16]. The temporal (inferior) horn of the left lateral ventricle and the cavum septum pellucidum (CSP) are two structures that have consistently been found enlarged in patients with these disorders [17-19]. In this study we found common variants of genes Neurexin1 (*NRXN1*), LDL receptor related protein 1B (*LRP1B*), and RAR-Related Orphan Receptor (*RORA*) associated with enlargement of these structures. A previous study by Rujescu et al. described rare structural genetic variants of *NRXN1* associated with Schizophrenia [20]. *NRXN1* encodes a large presynaptic transmembrane protein that binds neuroligins to calcium-dependent synaptic complexes in the central nervous system, and is also involved in the formation of synaptic contacts [21]. *LRP1B* is a candidate gene for Alzheimer's disease [22] and *RORA* is a candidate gene for PTSD [23].

bioRxiv preprint doi: https://doi.org/10.1101/175489; this version posted August 11, 2017. The copyright holder for this preprint (which was not certified by peer review) is the author/funder, who has granted bioRxiv a license to display the preprint in perpetuity. It is made available under aCC-BY-NC-ND 4.0 International license.

Results:

We identified 31 SNP markers with at least a suggestive genome-wide association (P < 1E-08) in 21 out of 463 total studied phenotypes in the B-SNIP first wave (B-SNIP1) sample, which contains 1,115 unrelated cases and controls genotyped using the Illumina Infinium Psycharray (PsychChip) followed by imputation to the 1000 Genomes reference panel, and filtered to work with common SNPs (MAF≥0.05) on the PLINK regression model GWAS. There were three significant results after Family-Wise Error Rate (FWER) correction (see Methods) in the CSF volumes phenotype group. The strict Bonferroni significance threshold after multiple testing for 463 phenotypes is P < 2.16E-11 which was exceeded by the same three top results. Here we tabulate results with the P < 1E-08 suggestive association threshold, but only discuss significant results. Complete GWAS results can be requested from the authors through the B-SNIP website (http://b-snip.org).

(Table 1 here)

Associations with Cerebrospinal Fluid volumes:

The most significant genome-wide P values observed were associated with two CSF volumetric phenotypes measured by FreeSurfer structural MRI: the volume of the temporal horn of left lateral ventricle was associated (P= 1.156E-11) with rs80262609, an intronic SNP of Neurexin1 gene (*NRXN1*) located at Chr.2p16.3 (Fig.1a); and the volume of the Cavum Septum Pellucidum (CSP) (Fig.1b) had P= 1.661E-11 in association with rs79543758, an intronic SNP of the LDL receptor-related protein 1B gene (*LRP1B*). This same phenotype also had a P= 1.72E-10 association with rs6494245, an intronic SNP of the RAR-Related Orphan Receptor A gene (*RORA*) (Fig.1.b.2), which is a PTSD candidate gene [23]. These two CSF volumetric variables showed significant differences between cases and controls in the studied sample: The temporal horn of left lateral ventricle (ANOVA P=0.01) and the CSP (ANOVA P=9.4E-05) were larger in cases (Figure 2). A post-hoc analysis using Quanto [24] calculated the power for these two top SNP findings as 0.62 and 0.57, and their effect sizes (Eta) were 0.249 and 0.265 respectively (Supplementary Table 4). Because of reported discrepancies in reports on the association of CSP with SZ [25, 26], we conducted a blind semi-quantitative verification of the Freesurfer results with a random selection of MRI images by experienced imaging scientists using manual measurements, obtaining a positive correlation between manual ratings and the FreeSurfer CSP quantitative output (FreeSurfer vs. Rater's Cronbach's Alpha=0.775 (P=4.37E-07).

(Figures 1 and 2 here)

Other suggestive GWAS results:

Associations with Local Gyrification Indices:

FreeSurfer-based Local Gyrification Indices (LGI) from 9 brain regions showed 13 suggestively significant associations. Four of them (left precentral, left postcentral, left paracentral, and left superior parietal LGIs) were suggestively associated with the Homo sapiens TAR (HIV-1) RNA binding protein 1 gene (*TARBP1*). Three of these LGIs and one additional region (left precentral, left postcentral, left paracentral and left superior frontal LGIs) had suggestive association with rs28689015, an intergenic SNP on Chr8q12.2; and the left frontal pole LGI with rs17812318, an intronic SNP of *LINC01182*, a long non-

bioRxiv preprint doi: https://doi.org/10.1101/175489; this version posted August 11, 2017. The copyright holder for this preprint (which was not certified by peer review) is the author/funder, who has granted bioRxiv a license to display the preprint in perpetuity. It is made available under aCC-BY-NC-ND 4.0 International license.

coding RNA. Four other LGI suggestive associations pointed to other intergenic regions with P<1E-08 (Table 1). Analysis of variance did not show significant differences between cases and controls or among diagnostic categories for these phenotypes.

Associations with Fractional Anisotropy:

Fractional Anisotropy (FA) is a metric of white matter fiber density and integrity, computed from Diffusion Tensor Imaging (DTI). FA of the left external capsule was suggestively associated (P=2.947E-09) with rs143413095, an intergenic SNP on Chr.9p23.3; and FA of the left cerebral peduncle had suggestively significant association (P=4.233E-09) with rs819605, an intergenic SNP on Chr.1p21.3. No significant differences between cases and controls were observed for these two variables.

Association with Age at Onset:

One clinical phenotype, the "Age of first symptoms of schizophrenia or bipolar disorder" reached suggestive significance association with rs1377950 (P=6.841E-09), however this did not pass the FWER significance threshold for psychiatric and medical history variables (Supplementary Table 1). This SNP is an intergenic marker on Chr.2p16.2, 300Kb from *LOC730100*, a long non-coding RNA neighbor of the *NRXN1* gene. A microRNA (*Mir4431*) has also been described adjacent to this locus. The CSP volume had a small but significant negative correlation with the age at onset in our sample (R= -0.118; P=3.89E-04).

Discussion:

Significant genetic associations with brain CSF volumetric variants related to psychotic disorders:

Cerebrospinal fluid volumes are some of the most reliable measurements captured with *in vivo* MRI, because of the high contrast between CSF and cerebral structures. Enlarged ventricular volumes have been among the most enduring anatomical findings in SZ and BD, first reported by Johnstone in schizophrenia forty years ago [27]. This has been confirmed in SZ and BD patients compared with healthy controls in large studies by the ENIGMA consortium [16, 28], and its heritability calculated as 0.54[29]. Increased ventricular volumes observed in schizophrenia have been attributed to volume reduction of surrounding grey matter structures [30, 31]. The temporal horn of the lateral ventricle traverses the temporal lobe and is in direct relation with the amygdala, hippocampus, and caudate nucleus. However, our GWAS on these structures' separate volumes did not have significant associations, which implies that the volumetric association may reflect joint regulation of part of the morphology of these structures. We noted that hippocampal volumes in our sample were significantly smaller in cases than in controls (ANOVA P=3E-06)[32-34], and there were also significant reductions in cases for the amygdala volumes (P=0.001), but not for the caudate. Gaser et al. reported ventricular enlargement in schizophrenia associated with volumetric reduction of the thalamus and superior temporal cortex [30]; in our data, however, we did not observe significant correlation between the volumes of these structures and the volume of the temporal horn of lateral ventricle, or any detectable associations between these structures volumes and the CSF volume-associated genes.

In our analyses we observed significantly larger volumes of the temporal horn of left lateral ventricle in cases vs. controls, and polymorphism in the Neurexin1 gene (*NRXN1*) was associated with this endophenotype. When we combined temporal horns values across hemispheres, the association was still suggestively significant (P=4.92E-10). The Psychiatric Genomic Consortium (PGC) reported an association P= 0.005685 for this same SNP marker of *NRXN1* (rs80262609) with diagnosis in their large

bioRxiv preprint doi: https://doi.org/10.1101/175489; this version posted August 11, 2017. The copyright holder for this preprint (which was not certified by peer review) is the author/funder, who has granted bioRxiv a license to display the preprint in perpetuity. It is made available under aCC-BY-NC-ND 4.0 International license.

case-control schizophrenia GWAS [1]. Structural variants (CNVs) disrupting this gene have been associated with a wide spectrum of brain disorders including schizophrenia [20, 35, 36], and with cognitive performance through the regulation of post-synaptic N-methyl d-aspartate receptors [37]. This gene is expressed in the adult brain[38], and during development in the fetal brain[39].

The cavum septum pellucidum is a space between the two leaflets of the septum pellucidum that normally occludes in 85% of babies by age 6 months[40]; its persistence has been related to neurodevelopmental delay[41], and with SZ and BD[17, 18, 42, 43], presumably because of a reduction of the limbic structures that surround it: the septal nuclei, fornix and hippocampal commissure. In our sample this quantitative phenotype measured in voxels by FreeSurfer was significantly different in cases vs. controls (ANOVA P=9.4E-05, Figure 2), with larger volumes for individuals with SZ than BP, which is consistent with findings from Shioiri et al. [18]. One of the genes identified in association with the CSP volume, the LDL receptor related protein 1B, has been associated with Attention Deficit/Hyperactivity Disorder and Alzheimer's disease [22, 44]. *LRP1B* is reported expressed in the adult and fetal brain[45] which, along with its association with an anatomical quantitative trait (CSP) of a persistent fetal structure, supports a role of this gene in a neurodevelopmental hypothesis of Bipolar Disorder and Schizophrenia [26]. *RORA* is a nuclear receptor that participates in the transcriptional regulation of some genes involved in circadian rhythm and in the response to lithium treatment in bipolar disorder[46]. In mice, RORα is essential for development of cerebellum through direct regulation of genes expressed in Purkinje cells.

According to UK Brain Expression Consortium (UKBEC) eQTL data (http://www.braineac.org/), rs80262609 is an eQTL SNP (P < 0.01) for *NRXN1* in putamen area, temporal cortex, frontal cortex, and thalamus (Supplementary Table 3), whereas rs6494245 is primarily an eQTL SNP for *VPS13C* in hippocampus, cerebellum, and occipital cortex; also associated with expression of *RORA* in hippocampus, frontal cortex, medulla, and thalamus; associated with *NARG2* expression in hippocampus, cerebellum, and frontal cortex; with *ANXA2* expression in hippocampus. Among these genes, *RORA* is a core transcription factor involving circadian rhythms. *VPS13C* involves mitochondrial function and maintenance of mitochondrial transmembrane potential. *NARG2* regulates small nuclear RNA (snRNA) gene transcription. *ANXA2* involves in exocytosis. Co-expression analysis of *NRXN1* and *LRP1B* using the Neuropsychiatric Disorder De Novo Mutations Database [47] identified genes involved in cell adhesion (including Cadherin13) and neurotransmission (including the Glutamate Ionotropic Receptor AMPA 2 (Supplementary Figure 3). Previously published B-SNIP analyses on a subset of this sample looking for gene networks associated with some of these phenotypes found cell adhesion networks containing CDH13, NRXN3 and *RORA* in association with EEG oscillations, event-related potentials, resting state fMRI and structural MRI phenotypes [12, 48-51]. Although not a replication because our data contains that subsample, this study may represent support for these previous studies with respect to CDH13 and *RORA*.

The significant genetic associations with volumes of the temporal horn of lateral ventricle and of the CSP represent novel genetic findings on the molecular basis of psychotic disorders, and are the first genetic associations with psychosis that pinpoint a stage of brain development by direct anatomic observation. The relationship between age of onset of psychosis and a ventricular volume, in the context of a significant genetic association for one of the two phenotypes and a suggestive association for the other, is the type of finding that gives credence to the B-SNIP consortium deep phenotyping approach study [2]. We have observed highly significant p-values with a relatively smaller sample size than needed for disease association, and relatively large effect sizes for the significant associations, which suggest that diagnosis may be a more difficult phenotype to study than some of its observable components.

bioRxiv preprint doi: https://doi.org/10.1101/175489; this version posted August 11, 2017. The copyright holder for this preprint (which was not certified by peer review) is the author/funder, who has granted bioRxiv a license to display the preprint in perpetuity. It is made available under aCC-BY-NC-ND 4.0 International license.

Methods:

The BSNIP1 data set: Data analyzed here comes from the Bipolar and Schizophrenia Network for Intermediate Phenotypes - first wave (B-SNIP1), which studied individuals with a history of psychosis and diagnoses of Schizophrenia, Bipolar, or Schizoaffective disorder (SAD) [52]. BSNIP-1 collected a comprehensive battery of phenotypes including clinical and behavioral interview data, cognitive trait assessments, oculo-motor testing with smooth pursuit and saccade paradigms, resting-state EEG, auditory-event-related potentials, and brain imaging (structural, diffusion tensor, resting state functional MRI). This comprehensive set of psychosis-related phenotypes was acquired between 2008 and 2012 from more than 2,400 individuals, including 312 BD with psychotic features, 223 SAD and 397 SZ cases, 1029 first degree relatives of cases, and 455 unrelated healthy controls following standardized methods in five different study sites in the USA, under IRB approval from each participating institution. Relatives were excluded from our GWAS analyses and only individuals that passed QC described below were included.

Phenotypes: Details of B-SNIP1 phenotype collection are described in Tamminga el al. 2014 [5], Diffusion Tensor Imaging was processed as in Skudlarski 2010[11], and structural neuroimaging variables extracted from MRI were processed using FreeSurfer version 5.1 [53] as described in Padmanabhan et al. 2015[10]. These phenotypes, assembled within the B-SNIP1 analytical database [5], were used as quantitative phenotypes for genome-wide association. Analyses were conducted on data from 1,115 unrelated patients and healthy control volunteers with available phenotypes and genotypes: of these 754 are cases (245 Bipolar, 186 Schizoaffective and 323 Schizophrenia) and 361 controls; 561 are males and 554 are females. 654 individuals self-reported as Caucasians, 375 as African Americans, and 86 self-reported other ethnicities (includes Asians, American Indian, Native Hawaiian, multiracial, others and unknown). The number of subjects analyzed for each trait varied, as only individuals with non-missing data were included for analysis and no phenotype imputation was applied. Phenotypes were inspected for accuracy and to detect outliers based on their values distribution. A total of 463 phenotypes were used for GWAS. Supplementary Table 1 shows a summary of phenotypes by groups, and the complete phenotype list is available in Supplementary Table 2. Although some variables exhibited high correlation with others like thickness, area and volumes from structural MRI cortical parcellations, genetic factors associated with each may be different and worth analyzing separately as stated by Winkler et al. [54].

Genotypes were assessed from blood DNA at the Broad Institute using the Illumina Infinium Psycharray (PsychChip), which contains a total of 588,454 SNP markers, including 50,000 specific genetic markers for neuropsychiatric disorders. PsychChip genotype calls were processed through a Broad Institute custom pipeline designed to merge calls from 3 different algorithms (GenCall, Birdseed and zCall), in order to maximize reliability and usability of rare markers [55]. Pre-Imputation QC applied to the called PsychChip genotypes included filtering by Call Rate > 98% by SNP and >98% by sample, HWE P-value > 1E-06 in controls, Inbreeding Coefficient (-0.2 > F_Het > 0.2), exclusion of monomorphic markers, Sex Check using X chromosome heterozygosity and Y chromosome call rate, and Minor Allele Frequency (MAF) 0.01. We used programs PREST-plus [56] and KING [57] to check genotypes of all putatively unrelated patient and control individuals for cryptic relatedness, so that the final dataset had no individuals who showed 3rd degree or closer kinship.

bioRxiv preprint doi: https://doi.org/10.1101/175489; this version posted August 11, 2017. The copyright holder for this preprint (which was not certified by peer review) is the author/funder, who has granted bioRxiv a license to display the preprint in perpetuity. It is made available under aCC-BY-NC-ND 4.0 International license.

Genotype Imputation: After QC, PsychChip genotypes were imputed to the 1000 Genomes project multiethnic reference panel [58] using HAPI-UR for pre-phasing and IMPUTE2 [59-61]. Chromosomes were phased separately, and then divided into 5 megabase pair chunks for imputation. Poorly imputed single nucleotide polymorphisms (SNPs) were filtered post-imputation. The final imputed genotype set contained more than 30 Million autosomal markers, reduced to 4,322,238 variants after filtering for 0.05 missingness by marker, 0.02 missingness by individual sample and MAF 0.05, to work with common variants.

GWAS analysis: were performed using PLINK 1.9 [62, 63] on the Bionimbus protected cloud of the Open Science Data Cloud servers at the University of Chicago [64](http://www.opensciencedatacloud.org). Genetic locations refer to the human genome GRCh37/hg19 build, gene mapping was done using the UCSC genome browser [65], and graphics generated with Manhattan Plotter[66] and LocusZoom[67]. Population stratification was expected in the B-SNIP1 sample, as it contains people from diverse ethnicities. We ran Principal Component Analysis (PCA) on the genotypes to examine population stratification and admixture in our sample (Supplementary Figure 1a). Then, the first two PCA eigenvectors which captured the vast majority of the ethnic-related variance (Supplementary Figure 1b) were used as covariates in the GWAS regression model to correct for population stratification and admixture [68]. Sex was also used as a covariate in all our analyses. Although recent publications use multiple additional covariates (like case-control status, age, total intracranial volume, etc.) [16, 69], in our study we explicitly avoided them because correcting for factors that are related to the disease could diminish the possibility of detecting associations with loci that differentiate cases and controls, or that are related to the evolution of the disease and that can thus be responsible for phenotypic variance. Where significant or suggestive gene associations were observed with a phenotype, analysis of variance (ANOVA) was used to test for significant case-control phenotypic differences, calculated with IBM SPSS Statistics version 24. Q-Q plots were used to examine possible inflation in GWAS results (Suppl. Figure 2).

Significance Thresholds: The classic definition of statistically suggestive and significant probability thresholds in whole genome analysis is that a result is suggestive if it is expected to occur not more than once in a single genome-wide analysis, and significant if it is expected to occur not more than once in the context of all the analyses under consideration[70]. The GWAS statistical significance threshold for a single phenotype analysis of imputed data using the 1000 Genomes reference panel is accepted as $P < 1E-08$, based on the number of effective markers (Li et al. [71]). In the context of the multiple analyses reported here, this would be our threshold for suggestive significance. Given the different classes of phenotype classes analyzed (psychiatric scales, clinical data, fractional anisotropy and structural MRI, we opted for a Family-Wise Error Rate (FWER) approach (considering each class of variable as a separate family) to correct for multiple testing and declare FWER significance (Supplementary Table 1). We note separately findings that pass a Bonferroni correction for all variables analyzed.

Grant support:

NIH/NIMH grant 5R01MH077862: Bipolar-Schizophrenia Consortium for parsing Intermediate Phenotypes. PI: Sweeney, John A. (BSNIP1).

bioRxiv preprint doi: https://doi.org/10.1101/175489; this version posted August 11, 2017. The copyright holder for this preprint (which was not certified by peer review) is the author/funder, who has granted bioRxiv a license to display the preprint in perpetuity. It is made available under aCC-BY-NC-ND 4.0 International license.

NIH/NIMH grant 5R01MH077851: Bipolar-Schizophrenia Network for Intermediate Phenotypes 2 (B-SNIP). PI: C Tamminga.

NIH/NIMH grant 5R01MH103368: Bipolar-Schizophrenia Network for Intermediate Phenotypes 2 (B-SNIP). PI: E. Gershon.

NIH/NIMH grant 5R01MH077945: Bipolar-Schizophrenia Network for Intermediate Phenotypes 2 (B-SNIP). PI: G. Pearlson.

NIH/NIMH grant 5R01MH078113: Bipolar-Schizophrenia Network for Intermediate Phenotypes 2 (B-SNIP . PI: M. Keshavan.

NIH/NIMH grant 5R01MH103366: Bipolar-Schizophrenia Network for Intermediate Phenotypes 2 (B-SNIP). PI: B. Clementz.

NIH/NIMH grant 5P50MH094267: Conte Center for Computational Systems Genomics of Neuropsychiatric Phenotypes. PI: A. Rzhetsky.

Disclosures:

Dr. Sweeney reports serving on an advisory board to Takeda. Dr. Keshavan has received a grant from Sunovion and is a consultant to Forum Pharmaceuticals. Dr. Tamminga is a consultant to Intracellular Therapies, an ad hoc consultant to Takeda and Astellas and received a grant from Sunovion. The other authors report no conflicts of interests.

Acknowledgments:

Thanks to the probands, their families and volunteers who joined this study and contributed their time and individual data.

This work made use of the Bionimbus Protected Data Cloud (PDC), which is a collaboration between the University of Chicago Center for Data Intensive Science (CDIS) and the Open Commons Consortium (OCC). The Bionimbus PDC allows users authorized by NIH to compute over human genomic data in a secure compliant fashion. The Bionimbus PDC is part of the OSDC ecosystem.

bioRxiv preprint doi: https://doi.org/10.1101/175489; this version posted August 11, 2017. The copyright holder for this preprint (which was not certified by peer review) is the author/funder, who has granted bioRxiv a license to display the preprint in perpetuity. It is made available under aCC-BY-NC-ND 4.0 International license.

REFERENCES

1. Schizophrenia Working Group of the Psychiatric Genomics, C., *Biological insights from 108 schizophrenia-associated genetic loci.* Nature, 2014. **511**(7510): p. 421-7.
2. Dahl, A., et al., *A multiple-phenotype imputation method for genetic studies.* Nat Genet, 2016. **48**(4): p. 466-72.
3. Bush, W.S. and J.H. Moore, *Chapter 11: Genome-wide association studies.* PLoS Comput Biol, 2012. **8**(12): p. e1002822.
4. Gronenschild, E.H., et al., *The effects of FreeSurfer version, workstation type, and Macintosh operating system version on anatomical volume and cortical thickness measurements.* PLoS One, 2012. **7**(6): p. e38234.
5. Tamminga, C.A., et al., *Bipolar and schizophrenia network for intermediate phenotypes: outcomes across the psychosis continuum.* Schizophr Bull, 2014. **40 Suppl 2**: p. S131-7.
6. Cuthbert, B.N. and T.R. Insel, *Toward the future of psychiatric diagnosis: the seven pillars of RDoC.* BMC Med, 2013. **11**: p. 126.
7. Arora, P. and C. Newton-Cheh, *Blood pressure and human genetic variation in the general population.* Curr Opin Cardiol, 2010. **25**(3): p. 229-37.
8. Doris, P.A., *The genetics of blood pressure and hypertension: the role of rare variation.* Cardiovasc Ther, 2011. **29**(1): p. 37-45.
9. Manolio, T.A., et al., *Finding the missing heritability of complex diseases.* Nature, 2009. **461**(7265): p. 747-53.
10. Padmanabhan, J.L., et al., *Correlations between brain structure and symptom dimensions of psychosis in schizophrenia, schizoaffective, and psychotic bipolar I disorders.* Schizophr Bull, 2015. **41**(1): p. 154-62.
11. Skudlarski, P., et al., *Diffusion tensor imaging white matter endophenotypes in patients with schizophrenia or psychotic bipolar disorder and their relatives.* Am J Psychiatry, 2013. **170**(8): p. 886-98.
12. Meda, S.A., et al., *Multivariate analysis reveals genetic associations of the resting default mode network in psychotic bipolar disorder and schizophrenia.* Proc Natl Acad Sci U S A, 2014. **111**(19): p. E2066-75.
13. International Schizophrenia, C., et al., *Common polygenic variation contributes to risk of schizophrenia and bipolar disorder.* Nature, 2009. **460**(7256): p. 748-52.
14. Franke, B., et al., *Genetic influences on schizophrenia and subcortical brain volumes: large-scale proof of concept.* Nat Neurosci, 2016. **19**(3): p. 420-431.
15. Strasser, H.C., et al., *Hippocampal and ventricular volumes in psychotic and nonpsychotic bipolar patients compared with schizophrenia patients and community control subjects: a pilot study.* Biol Psychiatry, 2005. **57**(6): p. 633-9.
16. Hibar, D.P., et al., *Subcortical volumetric abnormalities in bipolar disorder.* Mol Psychiatry, 2016. **21**(12): p. 1710-1716.
17. Galarza, M., et al., *Cavum septum pellucidum and its increased prevalence in schizophrenia: a neuroembryological classification.* J Neuropsychiatry Clin Neurosci, 2004. **16**(1): p. 41-6.
18. Shioiri, T., et al., *Prevalence of cavum septum pellucidum detected by MRI in patients with bipolar disorder, major depression and schizophrenia.* Psychol Med, 1996. **26**(2): p. 431-4.
19. DeLisi, L.E., et al., *Increased prevalence of cavum septum pellucidum in schizophrenia.* Psychiatry Res, 1993. **50**(3): p. 193-9.
20. Rujescu, D., et al., *Disruption of the neurexin 1 gene is associated with schizophrenia.* Human Molecular Genetics, 2009. **18**(5): p. 988-996.
21. Coordinators, N.R., *Database Resources of the National Center for Biotechnology Information.* Nucleic Acids Res, 2017. **45**(D1): p. D12-D17.
22. Shang, Z., et al., *Genome-wide haplotype association study identify TNFRSF1A, CASP7, LRP1B, CDH1 and TG genes associated with Alzheimer's disease in Caribbean Hispanic individuals.* Oncotarget, 2015. **6**(40): p. 42504-14.

bioRxiv preprint doi: https://doi.org/10.1101/175489; this version posted August 11, 2017. The copyright holder for this preprint (which was not certified by peer review) is the author/funder, who has granted bioRxiv a license to display the preprint in perpetuity. It is made available under aCC-BY-NC-ND 4.0 International license.

23. Logue, M.W., et al., *A genome-wide association study of post-traumatic stress disorder identifies the retinoid-related orphan receptor alpha (RORA) gene as a significant risk locus.* Mol Psychiatry, 2013. **18**(8): p. 937-42.
24. Gauderman, W.J., *Sample size requirements for matched case-control studies of gene-environment interaction.* Stat Med, 2002. **21**(1): p. 35-50.
25. Rajarethinam, R., et al., *No difference in the prevalence of cavum septum pellucidum (CSP) between first-episode schizophrenia patients, offspring of schizophrenia patients and healthy controls.* Schizophr Res, 2008. **103**(1-3): p. 22-5.
26. Khanra, S., et al., *Prevalence and Characteristics of Cavum Septum Pellucidum in Schizophrenia: A 16 Slice Computed Tomography Study.* Indian J Psychol Med, 2016. **38**(5): p. 455-459.
27. Johnstone, E.C., et al., *Cerebral ventricular size and cognitive impairment in chronic schizophrenia.* Lancet, 1976. **2**(7992): p. 924-6.
28. van Erp, T.G., et al., *Subcortical brain volume abnormalities in 2028 individuals with schizophrenia and 2540 healthy controls via the ENIGMA consortium.* Mol Psychiatry, 2016. **21**(4): p. 547-53.
29. Kremen, W.S., et al., *Heritability of brain ventricle volume: converging evidence from inconsistent results.* Neurobiol Aging, 2012. **33**(1): p. 1-8.
30. Gaser, C., et al., *Ventricular enlargement in schizophrenia related to volume reduction of the thalamus, striatum, and superior temporal cortex.* Am J Psychiatry, 2004. **161**(1): p. 154-6.
31. Degreef, G., et al., *Volumes of ventricular system subdivisions measured from magnetic resonance images in first-episode schizophrenic patients.* Arch Gen Psychiatry, 1992. **49**(7): p. 531-7.
32. Mathew, I., et al., *Medial temporal lobe structures and hippocampal subfields in psychotic disorders: findings from the Bipolar-Schizophrenia Network on Intermediate Phenotypes (B-SNIP) study.* JAMA Psychiatry, 2014. **71**(7): p. 769-77.
33. Ivleva, E.I., et al., *Brain Structure Biomarkers in the Psychosis Biotypes: Findings From the Bipolar-Schizophrenia Network for Intermediate Phenotypes.* Biol Psychiatry, 2017. **82**(1): p. 26-39.
34. Arnold, S.J., et al., *Hippocampal volume is reduced in schizophrenia and schizoaffective disorder but not in psychotic bipolar I disorder demonstrated by both manual tracing and automated parcellation (FreeSurfer).* Schizophr Bull, 2015. **41**(1): p. 233-49.
35. Schaaf, C.P., et al., *Phenotypic spectrum and genotype-phenotype correlations of NRXN1 exon deletions.* Eur J Hum Genet, 2012. **20**(12): p. 1240-7.
36. Duong, L., et al., *Mutations in NRXN1 in a family multiply affected with brain disorders: NRXN1 mutations and brain disorders.* Am J Med Genet B Neuropsychiatr Genet, 2012. **159B**(3): p. 354-8.
37. Davies, G., et al., *Genome-wide association study of cognitive functions and educational attainment in UK Biobank (N=112 151).* Mol Psychiatry, 2016. **21**(6): p. 758-67.
38. Carithers, L.J. and H.M. Moore, *The Genotype-Tissue Expression (GTEx) Project.* Biopreserv Biobank, 2015. **13**(5): p. 307-8.
39. Su, A.I., et al., *A gene atlas of the mouse and human protein-encoding transcriptomes.* Proc Natl Acad Sci U S A, 2004. **101**(16): p. 6062-7.
40. Saba, L., et al., *MR and CT of brain's cava.* J Neuroimaging, 2013. **23**(3): p. 326-35.
41. Bodensteiner, J.B., G.B. Schaefer, and J.M. Craft, *Cavum septi pellucidi and cavum vergae in normal and developmentally delayed populations.* J Child Neurol, 1998. **13**(3): p. 120-1.
42. Takahashi, T., et al., *Adhesio interthalamica in individuals at high-risk for developing psychosis and patients with psychotic disorders.* Prog Neuropsychopharmacol Biol Psychiatry, 2008. **32**(7): p. 1708-14.
43. de Souza Crippa, J.A., et al., *Cavum septum pellucidum and adhesio interthalamica in schizophrenia: an MRI study.* Eur Psychiatry, 2006. **21**(5): p. 291-9.
44. Poelmans, G., et al., *Integrated Genome-Wide Association Study Findings: Identification of a Neurodevelopmental Network for Attention Deficit Hyperactivity Disorder.* American Journal of Psychiatry, 2011. **168**(4): p. 365-377.

bioRxiv preprint doi: https://doi.org/10.1101/175489; this version posted August 11, 2017. The copyright holder for this preprint (which was not certified by peer review) is the author/funder, who has granted bioRxiv a license to display the preprint in perpetuity. It is made available under aCC-BY-NC-ND 4.0 International license.

45. Liu, C.X., et al., *The putative tumor suppressor LRP1B, a novel member of the low density lipoprotein (LDL) receptor family, exhibits both overlapping and distinct properties with the LDL receptor-related protein.* J Biol Chem, 2001. **276**(31): p. 28889-96.
46. McCarthy, M.J., et al., *A survey of genomic studies supports association of circadian clock genes with bipolar disorder spectrum illnesses and lithium response.* PLoS One, 2012. **7**(2): p. e32091.
47. Li, J., et al., *Genes with de novo mutations are shared by four neuropsychiatric disorders discovered from NPdenovo database.* Mol Psychiatry, 2016. **21**(2): p. 290-7.
48. Tandon, N., et al., *Novel gene-brain structure relationships in psychotic disorder revealed using parallel independent component analyses.* Schizophr Res, 2017. **182**: p. 74-83.
49. Mokhtari, M., et al., *Multivariate Genetic Correlates of the Auditory Paired Stimuli-Based P2 Event-Related Potential in the Psychosis Dimension From the BSNIP Study.* Schizophr Bull, 2016. **42**(3): p. 851-62.
50. Narayanan, B., et al., *Genetic Sources of Subcomponents of Event-Related Potential in the Dimension of Psychosis Analyzed From the B-SNIP Study.* Am J Psychiatry, 2015. **172**(5): p. 466-78.
51. Narayanan, B., et al., *Multivariate genetic determinants of EEG oscillations in schizophrenia and psychotic bipolar disorder from the BSNIP study.* Transl Psychiatry, 2015. **5**: p. e588.
52. Tamminga, C.A., et al., *Clinical phenotypes of psychosis in the Bipolar-Schizophrenia Network on Intermediate Phenotypes (B-SNIP).* Am J Psychiatry, 2013. **170**(11): p. 1263-74.
53. Fischl, B., *FreeSurfer.* Neuroimage, 2012. **62**(2): p. 774-81.
54. Winkler, A.M., et al., *Cortical thickness or grey matter volume? The importance of selecting the phenotype for imaging genetics studies.* Neuroimage, 2010. **53**(3): p. 1135-46.
55. Institute, T.B. 2016; Available from: https://sites.google.com/a/broadinstitute.org/psych-chip-resources/home.
56. Sun, L. and A. Dimitromanolakis, *PREST-plus identifies pedigree errors and cryptic relatedness in the GAW18 sample using genome-wide SNP data.* BMC Proc, 2014. **8**(Suppl 1 Genetic Analysis Workshop 18Vanessa Olmo): p. S23.
57. Manichaikul, A., et al., *Robust relationship inference in genome-wide association studies.* Bioinformatics, 2010. **26**(22): p. 2867-73.
58. Genomes Project, C., et al., *An integrated map of genetic variation from 1,092 human genomes.* Nature, 2012. **491**(7422): p. 56-65.
59. Williams, A.L., et al., *Phasing of many thousands of genotyped samples.* Am J Hum Genet, 2012. **91**(2): p. 238-51.
60. Howie, B., et al., *Fast and accurate genotype imputation in genome-wide association studies through pre-phasing.* Nat Genet, 2012. **44**(8): p. 955-9.
61. Howie, B.N., P. Donnelly, and J. Marchini, *A flexible and accurate genotype imputation method for the next generation of genome-wide association studies.* PLoS Genet, 2009. **5**(6): p. e1000529.
62. Chang, C.C., et al., *Second-generation PLINK: rising to the challenge of larger and richer datasets.* Gigascience, 2015. **4**: p. 7.
63. Purcell, S., et al., *PLINK: a tool set for whole-genome association and population-based linkage analyses.* Am J Hum Genet, 2007. **81**(3): p. 559-75.
64. Heath, A.P., et al., *Bionimbus: a cloud for managing, analyzing and sharing large genomics datasets.* J Am Med Inform Assoc, 2014. **21**(6): p. 969-75.
65. Kent, W.J., et al., *The human genome browser at UCSC.* Genome Res, 2002. **12**(6): p. 996-1006.
66. Morcillo, C. *Manhattan Plotter*. [cited 2017; Available from: http://www.biologiaevolutiva.org/~cmorcillo/tools/ManhattanPlotter/ManhattanPlotter.htm.
67. Pruim, R.J., et al., *LocusZoom: regional visualization of genome-wide association scan results.* Bioinformatics, 2010. **26**(18): p. 2336-7.
68. Price, A.L., et al., *Principal components analysis corrects for stratification in genome-wide association studies.* Nat Genet, 2006. **38**(8): p. 904-9.
69. Hibar, D.P., et al., *Novel genetic loci associated with hippocampal volume.* Nat Commun, 2017. **8**: p. 13624.

bioRxiv preprint doi: https://doi.org/10.1101/175489; this version posted August 11, 2017. The copyright holder for this preprint (which was not certified by peer review) is the author/funder, who has granted bioRxiv a license to display the preprint in perpetuity. It is made available under aCC-BY-NC-ND 4.0 International license.

70. Lander, E. and L. Kruglyak, *Genetic dissection of complex traits: guidelines for interpreting and reporting linkage results.* Nat Genet, 1995. **11**(3): p. 241-7.
71. Li, M.X., et al., *Evaluating the effective numbers of independent tests and significant p-value thresholds in commercial genotyping arrays and public imputation reference datasets.* Hum Genet, 2012. **131**(5): p. 747-56.
72. Faul, F., et al., *G*Power 3: a flexible statistical power analysis program for the social, behavioral, and biomedical sciences.* Behav Res Methods, 2007. **39**(2): p. 175-91.

bioRxiv preprint doi: https://doi.org/10.1101/175489; this version posted August 11, 2017. The copyright holder for this preprint (which was not certified by peer review) is the author/funder, who has granted bioRxiv a license to display the preprint in perpetuity. It is made available under aCC-BY-NC-ND 4.0 International license.

Table 1: Genome-Wide Association results:

CHR	BP	SNP	P	Gene	Phenotype
Associations with Cerebrospinal Fluid volumes					
2	**50,494,711**	**rs80262609**	**1.156E-11***	***NRXN1***	**Temporal horn of left lateral ventricle**
8	4,906,646	rs28689836	7.54E-09	*-intergenic-*	Temporal horn of left lateral ventricle
2	**141,420,560**	**rs79543758**	**1.661E-11***	***LRP1B***	**Cavum Septum Pellucidum volume**
15	**61,331,429**	**rs6494245**	**1.72E-10***	***RORA***	**Cavum Septum Pellucidum volume**
6	166,505,823	rs60447583	2.24E-09	*-intergenic-*	Cavum Septum Pellucidum volume
16	78,131,472	rs113700777	8.49E-09	*-intergenic-*	Cavum Septum Pellucidum volume
Association with Local Gyrification Indices					
4	13,879,341	rs17812318	8.98E-10	*LOC101929071*	Left frontal pole local gyrification index
8	62,187,789	rs28689015	1.38E-09	*-intergenic-*	Left paracentral local gyrification index
14	38,702,361	rs10498339	5.80E-09	*-intergenic-*	Left paracentral local gyrification index
9	33,451,929	rs111641181	6.54E-09	*-intergenic-*	Left paracentral local gyrification index
1	234,556,362	rs61825881	6.63E-09	*TARBP1*	Left paracentral local gyrification index
11	134,765,455	rs78485315	1.59E-09	*-intergenic-*	Left pericalcarine local gyrification index
1	234,556,362	rs61825881	3.93E-09	*TARBP1*	Left postcentral local gyrification index
8	62,187,789	rs28689015	6.44E-09	*-intergenic-*	Left postcentral local gyrification index
1	234,556,362	rs61825881	3.36E-10	*TARBP1*	Left precentral local gyrification index
8	62,187,789	rs28689015	1.07E-09	*-intergenic-*	Left precentral local gyrification index
9	33,451,929	rs111641181	6.59E-09	*-intergenic-*	Left precentral local gyrification index
14	38,702,361	rs10498339	5.35E-09	*-intergenic-*	Left rostral middle frontal local gyrification index
8	62,187,789	rs28689015	2.64E-10	*-intergenic-*	Left superior frontal local gyrification index
1	234,556,362	rs61825881	2.46E-09	*TARBP1*	Left superior parietal local gyrification index
14	38,702,361	rs10498339	9.08E-09	*-intergenic-*	Left frontal pole local gyrification index
8	62,078,904	rs6471932	8.72E-09	*-intergenic-*	Left precentral local gyrification index
8	84,969,532	rs72694334	7.30E-09	*-intergenic-*	Left superior frontal local gyrification index
6	139,842,563	rs653468	8.96E-09	*-intergenic-*	Right posterior cingulate local gyrification index
Associations with Fractional Anisotropy (Diffusion Tensor Imaging)					
9	16,087,032	rs143413095	2.95E-09	*-intergenic-*	Fractional Anisotropy: Left external capsule
1	99,633,193	rs819605	4.23E-09	*-intergenic-*	Fractional Anisotropy: Left cerebral peduncle
Associations with White Matter volumes					
22	42,347,391	rs11913578	6.91E-09	*-intergenic-*	Isthmus cingulate white matter volume
Associations with Grey Matter cortical parcellations					
18	339,337	rs17548440	8.97E-09	*COLEC12*	Left temporal pole volume
5	2,588,264	rs225752	7.77E-09	*-intergenic-*	Left caudal anterior cingulate volume
17	44,204,373	rs116392352	1.28E-09	*KANSL1*	Right pericalcarine area
Associations with Clinical Phenotypes					
2	52,969,757	rs1377950	6.84E-09	*-intergenic-*	Age of first SZ/BP Disorder symptoms

This table contains all significant and suggestive-significant GWAS results (P < 1E-08).

***:** P values that surpassed the Family-Wise Error Rate (FWER) significance threshold.

Bold font: P values significant after Bonferroni correction for 465 phenotypes (Bonf. α = 2.16E-11).

bioRxiv preprint doi: https://doi.org/10.1101/175489; this version posted August 11, 2017. The copyright holder for this preprint (which was not certified by peer review) is the author/funder, who has granted bioRxiv a license to display the preprint in perpetuity. It is made available under aCC-BY-NC-ND 4.0 International license.

Figure 1: Manhattan plots of top GWAS results:

a.- Volume of the temporal horn of left lateral ventricle

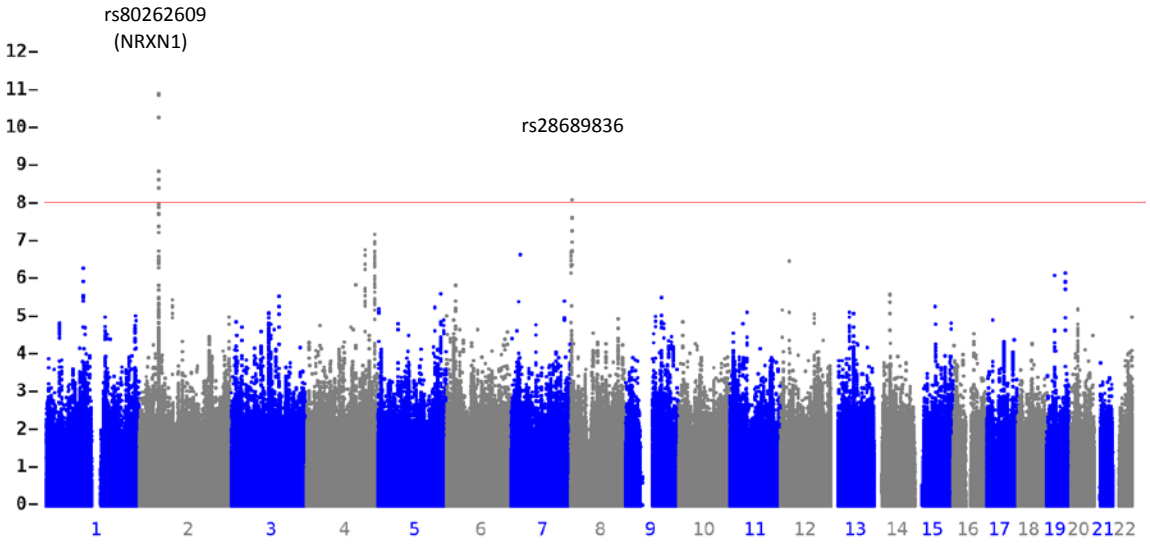

a.1.- Detail of Chromosome 2 region:

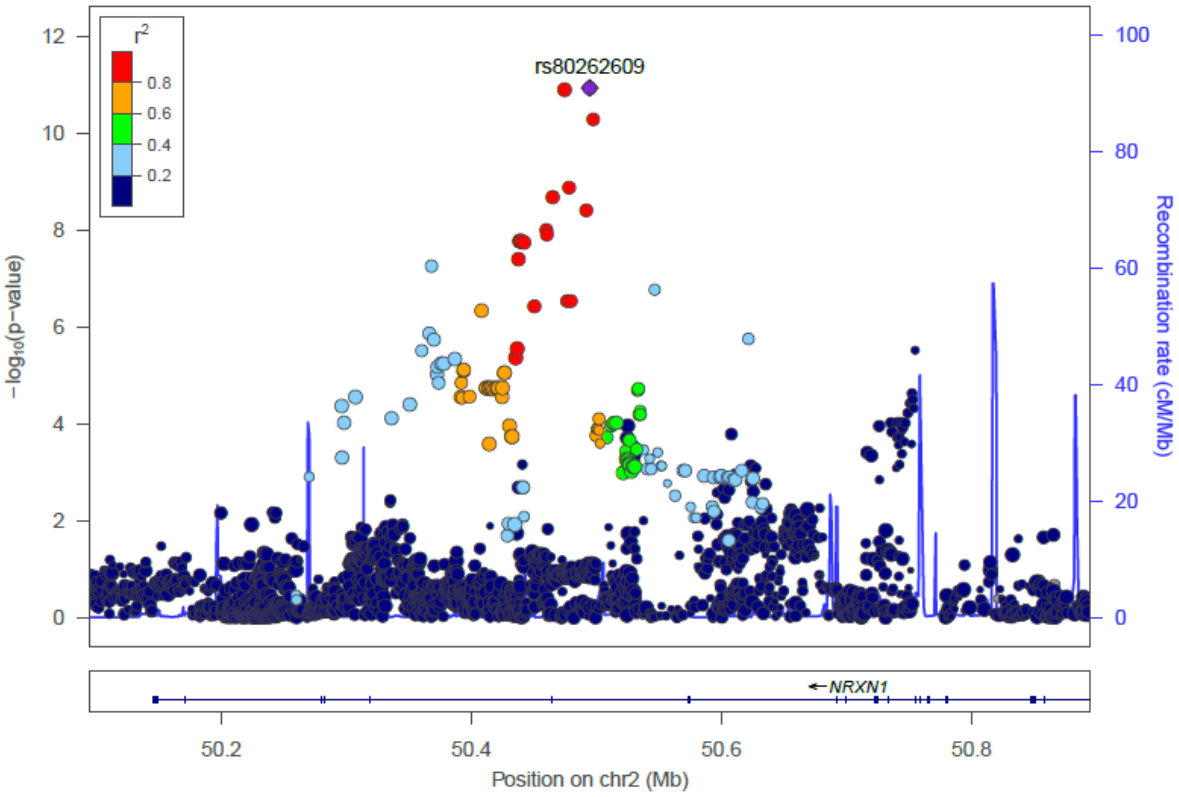

bioRxiv preprint doi: https://doi.org/10.1101/175489; this version posted August 11, 2017. The copyright holder for this preprint (which was not certified by peer review) is the author/funder, who has granted bioRxiv a license to display the preprint in perpetuity. It is made available under aCC-BY-NC-ND 4.0 International license.

b.- Cavum Septum Pellucidum volume

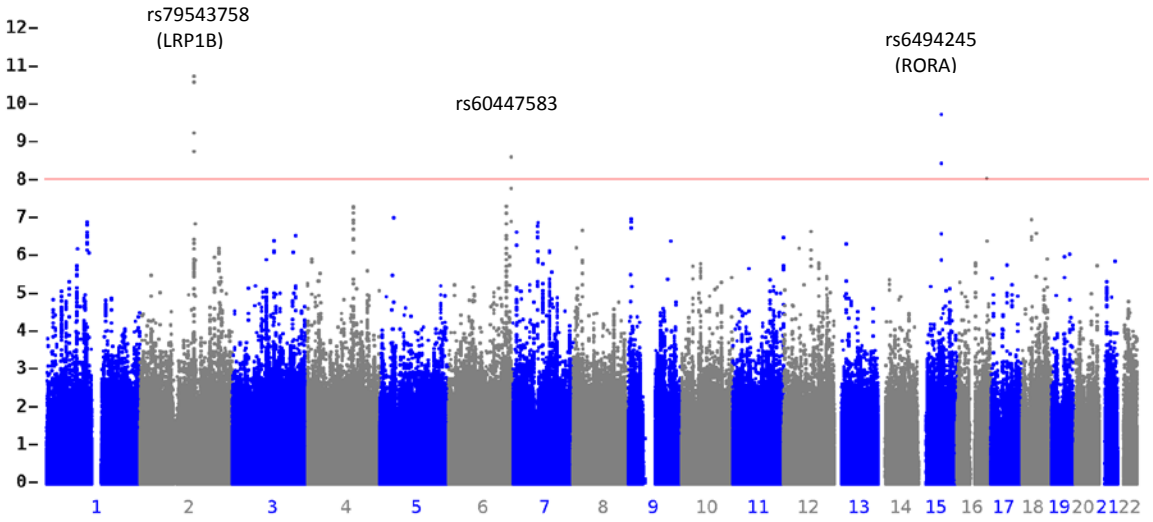

b.1.- Detail of Chromosome 2 region:

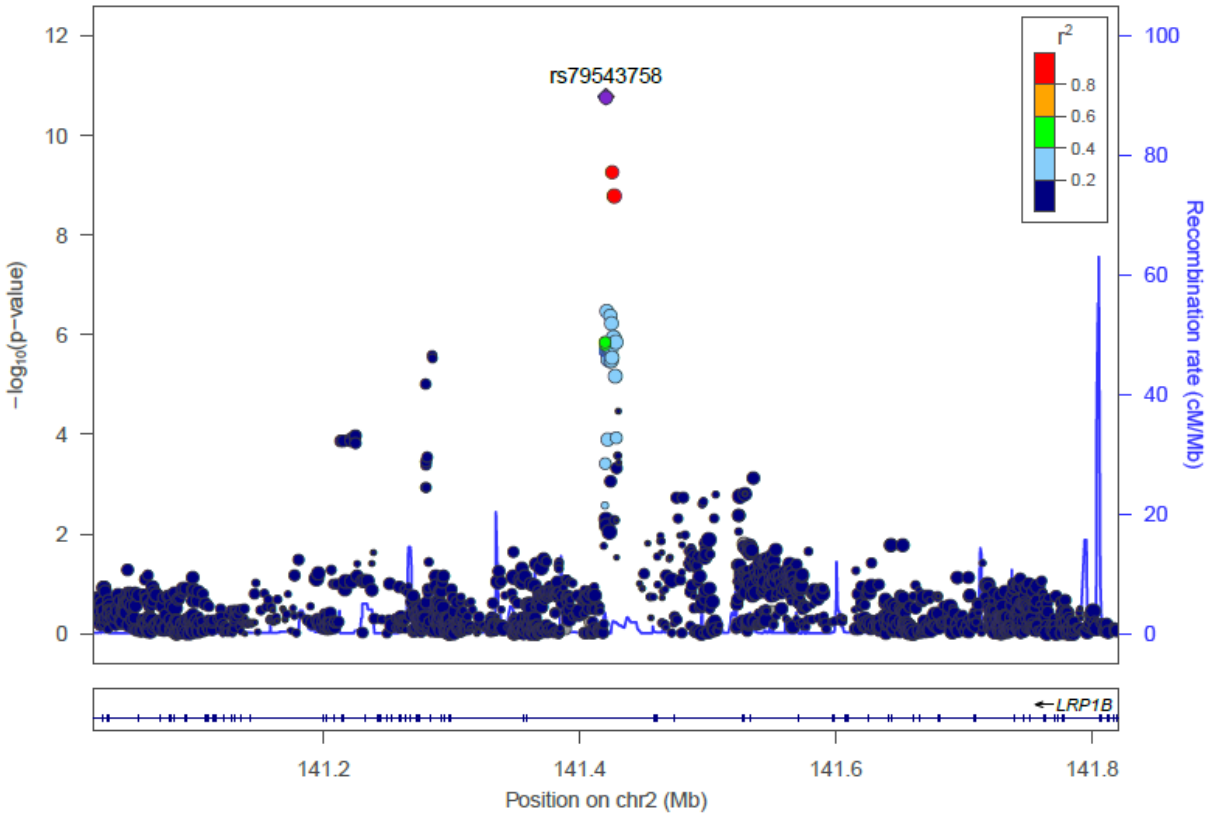

bioRxiv preprint doi: https://doi.org/10.1101/175489; this version posted August 11, 2017. The copyright holder for this preprint (which was not certified by peer review) is the author/funder, who has granted bioRxiv a license to display the preprint in perpetuity. It is made available under aCC-BY-NC-ND 4.0 International license.

b.2.- Detail of Chromosome 15 region:

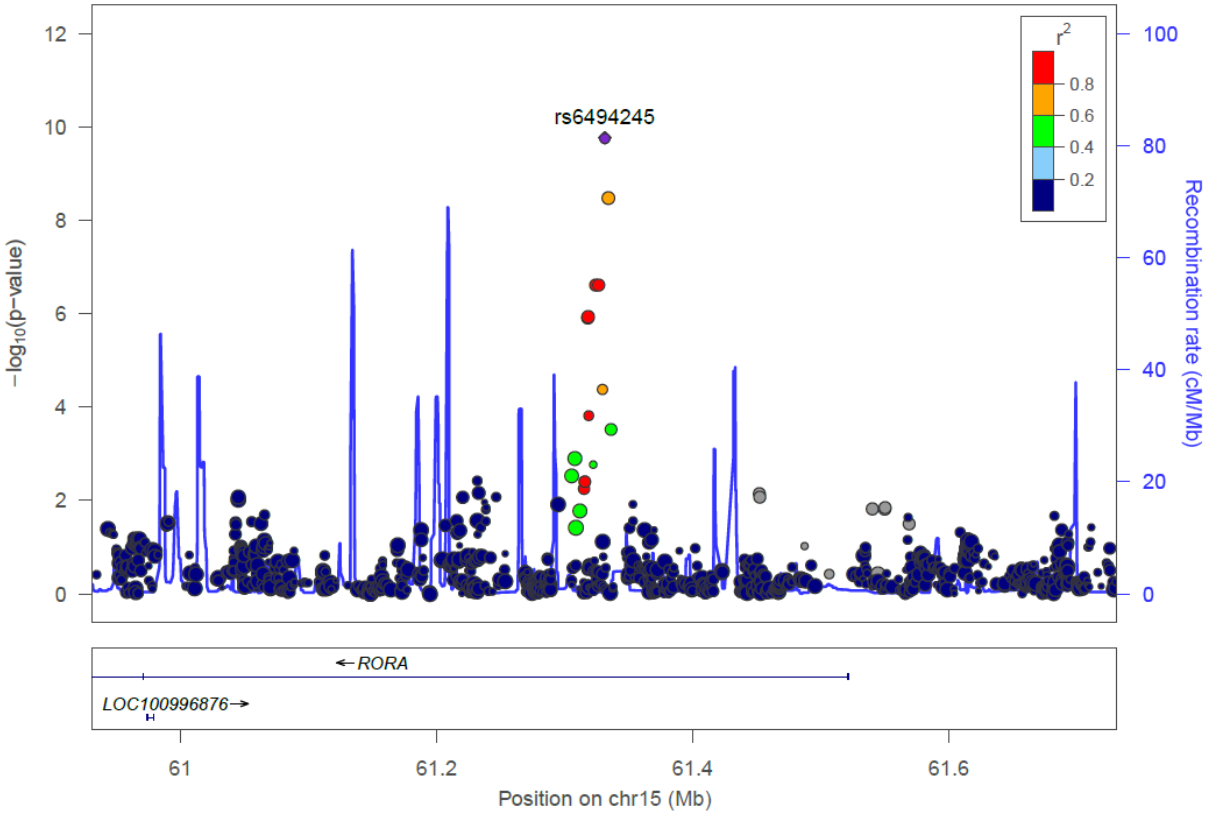

bioRxiv preprint doi: https://doi.org/10.1101/175489; this version posted August 11, 2017. The copyright holder for this preprint (which was not certified by peer review) is the author/funder, who has granted bioRxiv a license to display the preprint in perpetuity. It is made available under aCC-BY-NC-ND 4.0 International license.

Figure 2: Cavum Septum Pellucidum volume distribution in Cases and Controls

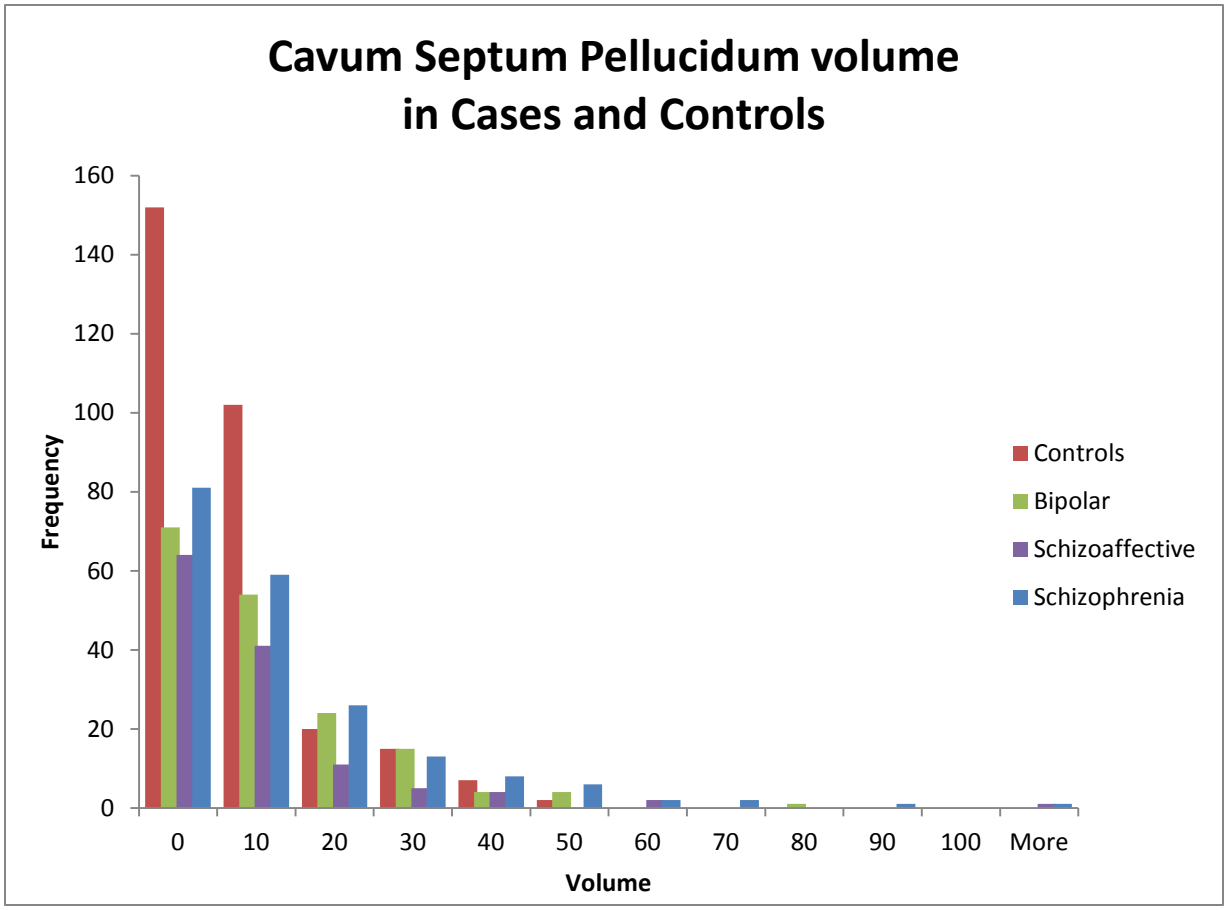

The distribution of CSP volumes (in Voxels) in cases and controls by diagnostic categories identified significant differences between groups (ANOVA P=9.4E-05).

bioRxiv preprint doi: https://doi.org/10.1101/175489; this version posted August 11, 2017. The copyright holder for this preprint (which was not certified by peer review) is the author/funder, who has granted bioRxiv a license to display the preprint in perpetuity. It is made available under aCC-BY-NC-ND 4.0 International license.

SUPPLEMENTARY MATERIAL

bioRxiv preprint doi: https://doi.org/10.1101/175489; this version posted August 11, 2017. The copyright holder for this preprint (which was not certified by peer review) is the author/funder, who has granted bioRxiv a license to display the preprint in perpetuity. It is made available under aCC-BY-NC-ND 4.0 International license.

Supplementary Table 1:

Family-Wise Error Rate significance threshold by phenotype groups

Phenotype Groups	Number of Phenotypes	FWER α	FWER Significant Results
1.- Psychiatric Scales	**15**	6.25E-10	-
2.- Psychiatric and Medical History	**4**	2E-09	-
3.- Fractional Anisotropy, DTI	**50**	2E-10	-
4- FreeSurfer structural MRI	**377**	2.65E-11	
CSF volumes	7	1.43E-09	3
Cortical parcellations LOCAL GYRIFICATION INDICES	68	1.47E-10	-
Grey Matter Cortical parcellations AREAS	70	1.43E-10	-
Grey Matter Cortical parcellations THICKNESS	68	1.47E-10	-
Grey Matter Cortical parcellations VOLUMES	68	1.47E-10	-
Sub-Cortical Structures AREAS	2	5E-09	-
Sub-Cortical Structures VOLUMES	12	8.33E-10	-
White Matter Cortical parcellations VOLUMES	68	1.47E-10	-
White Matter	6	1.67E-09	-
Cerebellum	4	2.5E-09	-
Others	4	2.5E-09	-
Additional FreeSurfer global variables:	**17**		
Total CSF volume	1	1E-08	-
Grey Matter	5	2E-09	-
Large brain structures	6	1.67E-09	-
White Matter	5	2E-09	-
All Phenotypes (Bonferroni)	**463**	**2.16E-11**	**3**

Complete list of phenotypes included in each group is available in Supplementary Table 2.

bioRxiv preprint doi: https://doi.org/10.1101/175489; this version posted August 11, 2017. The copyright holder for this preprint (which was not certified by peer review) is the author/funder, who has granted bioRxiv a license to display the preprint in perpetuity. It is made available under aCC-BY-NC-ND 4.0 International license.

Supplementary Table 2: Phenotype list

Download it from:
https://drive.google.com/file/d/0B_abC_nlCXwHMnl6SThsWXYwRG8/view?usp=sharing

Supplementary Table 3: eQTL analysis

Download it from:
https://drive.google.com/file/d/0B_abC_nlCXwHc29FdHlGZGpKVGc/view?usp=sharing

Supplementary Table 4: Power Analysis for top SNP findings:

Phenotype	Marker	N	MAF	Effect Size	Power
Temp Horn Left Lat Ventr	rs80262609	789	0.0538	0.249	0.62
CSP	rs79543758	784	0.0554	0.265	0.57

Power analysis for top SNPs in BSNIP GWAS using significance threshold = 1.78E-11, calculated with SPSS, Quanto and verified with G*Power[72].

bioRxiv preprint doi: https://doi.org/10.1101/175489; this version posted August 11, 2017. The copyright holder for this preprint (which was not certified by peer review) is the author/funder, who has granted bioRxiv a license to display the preprint in perpetuity. It is made available under aCC-BY-NC-ND 4.0 International license.

Supplementary Figure 1a: Principal Component Analysis (PCA) of genotypes showing population stratification.

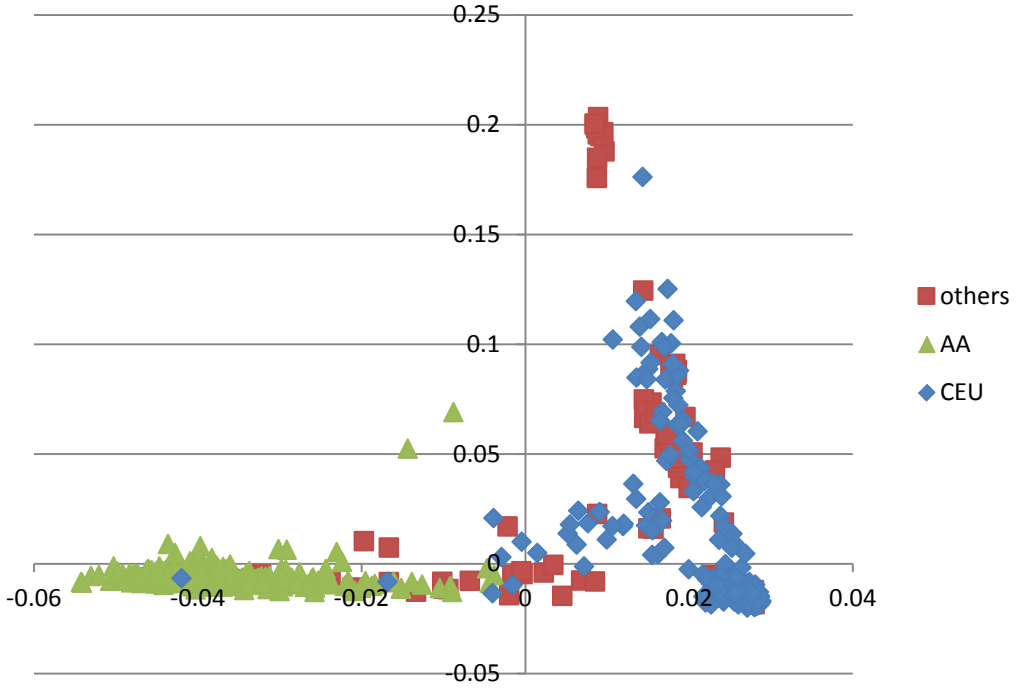

Genotype's PCA vs. Self-Reported ethnicity: Plot of the 2 first Eigenvectors from Principal Component Analysis (PCA) of genotypes: lower left corner cluster corresponds to African ancestry (AA), lower right corner cluster to Caucasian ancestry (CEU), and the upper middle to Asian ancestry component. Color code is self-reported ethnicity.

Supplementary Figure 1b: Plot of Eigenvalues from Genotypes' PCA, showing the variance captured by each Eigenvector.

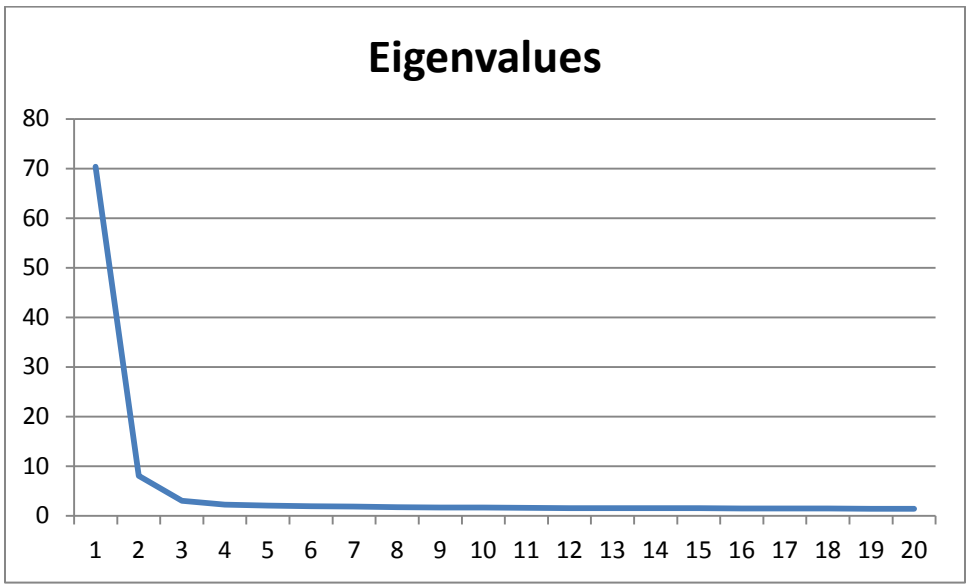

The two first Eigenvectors, which captured the majority of ethnic-related variance were used as covariates for GWAS.

bioRxiv preprint doi: https://doi.org/10.1101/175489; this version posted August 11, 2017. The copyright holder for this preprint (which was not certified by peer review) is the author/funder, who has granted bioRxiv a license to display the preprint in perpetuity. It is made available under aCC-BY-NC-ND 4.0 International license.

Supplementary Figure 2: GWAS Quantile-Quantile plots for highlighted phenotypes

a.- Volume of the temporal horn of left lateral ventricle

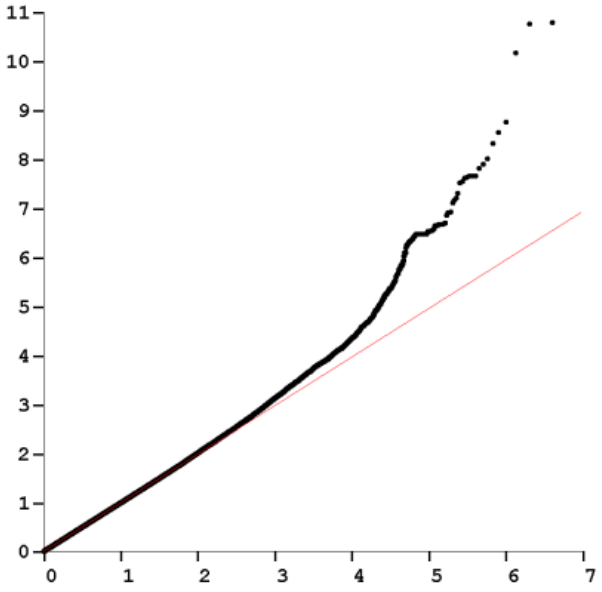

b.- Cavum Septum Pellucidum volume

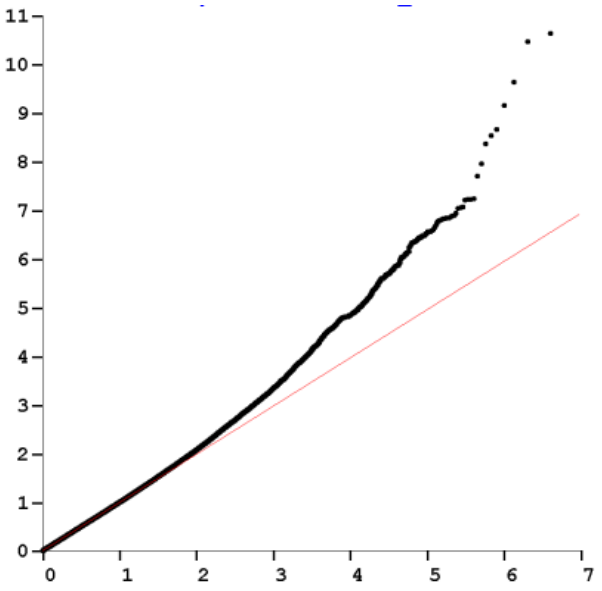

The red line represents the null distribution

bioRxiv preprint doi: https://doi.org/10.1101/175489; this version posted August 11, 2017. The copyright holder for this preprint (which was not certified by peer review) is the author/funder, who has granted bioRxiv a license to display the preprint in perpetuity. It is made available under aCC-BY-NC-ND 4.0 International license.

Supplementary Figure 3:

a. Co-expression Analysis of NRXN1, LRP1B and RORA

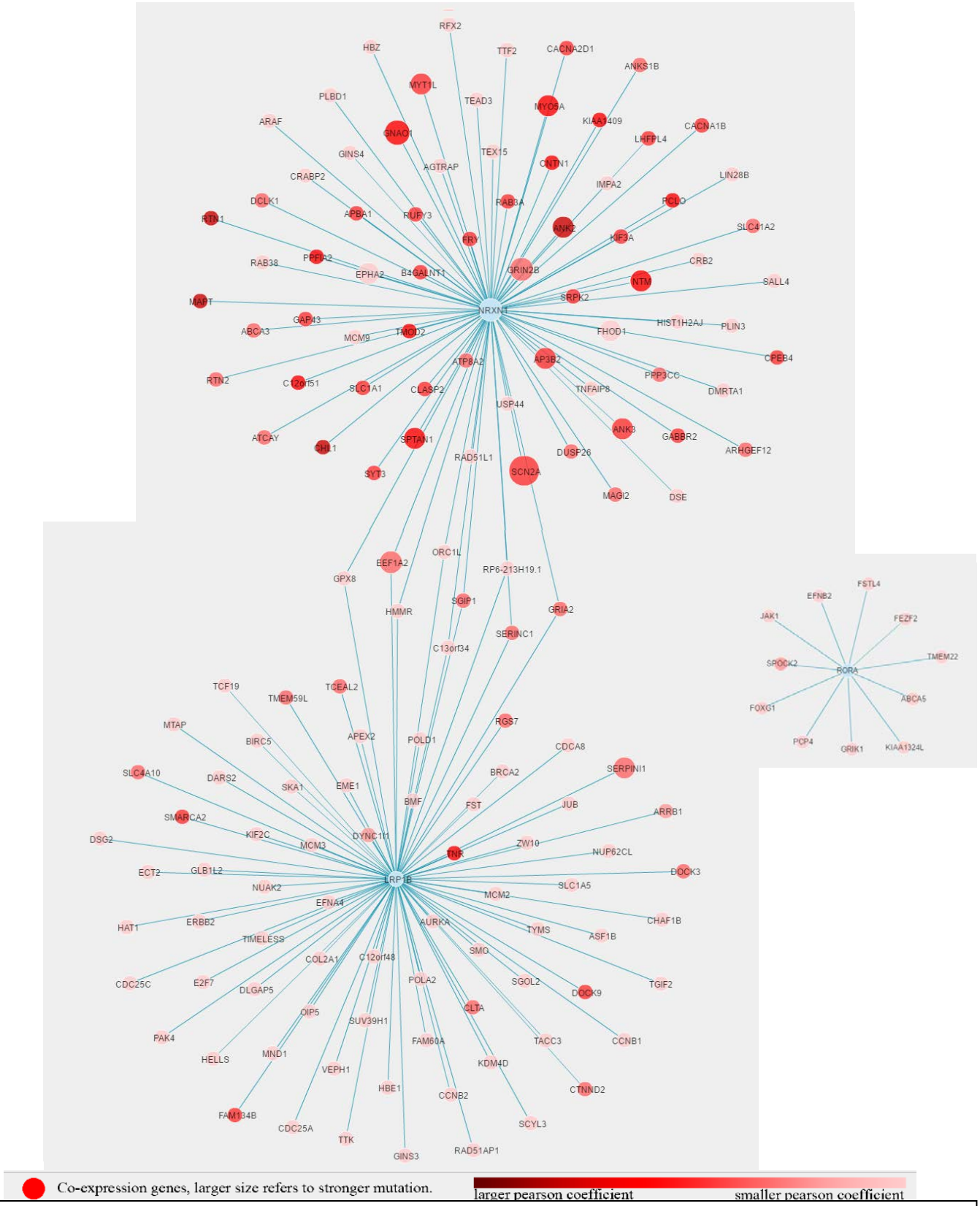

Co-expression analysis of the 3 genes associated with ventricular enlargement (NRXN1, LRP1B and RORA), using NPdenovo Co-expression analysis (http://www.wzgenomics.cn/NPdenovo/index.php). Reference Dataset: HBT; Minimum Pearson correlation coefficient: 0.8; Maximum nodes of network: 80. Several genes are co-expressed by NRXN1 and LRP1B, including GRIA2. No co-expression with RORA.

bioRxiv preprint doi: https://doi.org/10.1101/175489; this version posted August 11, 2017. The copyright holder for this preprint (which was not certified by peer review) is the author/funder, who has granted bioRxiv a license to display the preprint in perpetuity. It is made available under aCC-BY-NC-ND 4.0 International license.

b. Additional Co-expression Analysis of NRXN1 and LRP1B

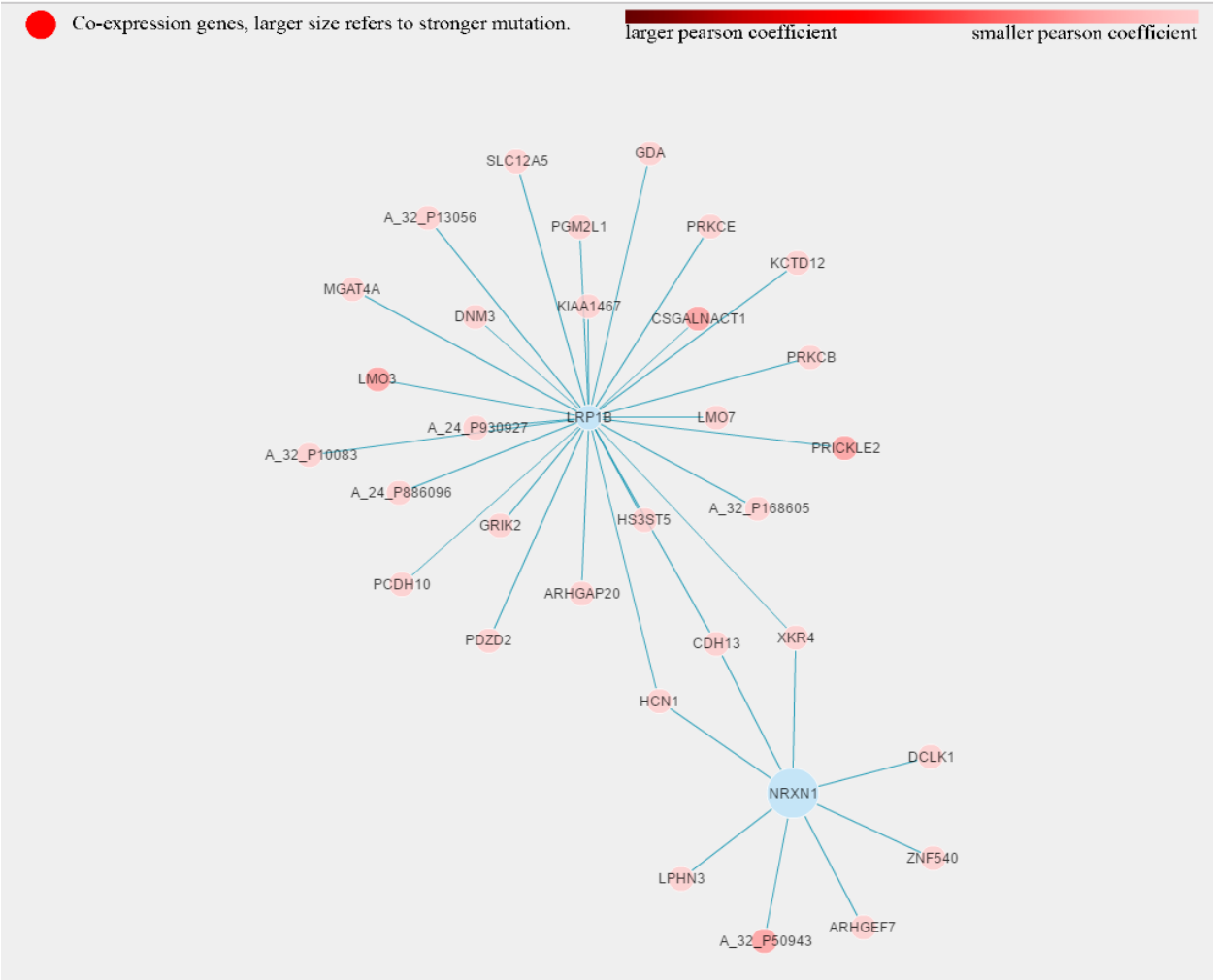

Secondary Co-expression analysis of NRXN1 and LRP1B on NPdenovo Co-expression analysis (http://www.wzgenomics.cn/NPdenovo/index.php), using Dataset: LMD, Minimum Pearson correlation coefficient: 0.8 Maximum nodes of network: 80. Cadherin 13 (along with 2 other genes) is identified in this dataset as a co-expressed gene.